CHINESE JOURNAL OF PHYSICS VOL. 52, NO. 2 April 2014

Prediction Study of Structural, Elastic, and Thermal Properties under the Pressure Effect of $CuMnPt_6$

Shuo Huang,* Rui-Zi Li, Chuan-Hui Zhang, and Jiang Shen

Department of Physics, University of Science and Technology Beijing, Beijing 100083, People's Republic China

(Received June 4, 2013)

The structural, elastic, and thermal properties of ABC_6-type $CuMnPt_6$ are studied up to 60 GPa with the first-principles pseudopotential method within the generalized gradient approximation. Our calculated results agree quite well with the comparable experimental data. The three principle elastic tensor elements (C_{11}, C_{12}, and C_{44}), and various secondary elasticity parameters, such as the bulk/shear elastic modulus, elastic anisotropy, and normalized elastic constants, as function of pressure are obtained and analyzed for the first time. The thermal properties, including the Debye temperature, Grüneisen constant, thermal expansion, and heat capacity, are also estimated at various pressures and temperatures.

DOI: 10.6122/CJP.52.891 PACS numbers: 61.66.Dk, 62.20.-x, 65.40.De

I. INTRODUCTION

Platinum when alloyed with 3*d*-transition metals strongly affects their ordering behaviors and hence their physical performance [1]. For example, Pt 14.at% Cu increases significantly in hardness as a result of the formation of ordered $CuPt_7$ domains [2]. The ferromagnetic $L1_2$ phase of the $MnPt_3$ compound exhibits a giant magneto-optical Kerr effect [3]. Further, it was reported that $MnPt_7$ also shows the $CuPt_7$ structure [4, 5], and Káňa *et al.* [6] predicted an antiferromagnetic state with spins altering along the [1 0 0] direction to be the ground state of this compound. What is more interesting is that Das *et al.* [7] have found that the ternary addition of Mn to $CuPt_3$ leads to a complete miscibility, without changing the ABC_6 type structure via the double-step ordering from the face-centered cubic (FCC) phase. The ABC_6 ordered structure, which is closely related to the $L1_2$ and $CuPt_7$ structure, can be described with the help of a $2 \times 2 \times 2$ Pt supercell with Cu and Mn atoms occupying alternate corner positions in the FCC lattice, as shown in Fig. 1.

Due to the notable ordering behavior, much effort has been paid to understand the physical properties of $CuMnPt_6$, which was regarded as a counterpart of the Heusler alloy forming in the body-centered cubic (BCC) systems [8]. Experimentally, the atomic arrangements in $CuMnPt_6$ at various temperatures were studied by in situ pulsed-neutron diffraction measurements [9]. A secondary ordering in the alloy was also discussed in terms

*Electronic address: shuogy@163.com

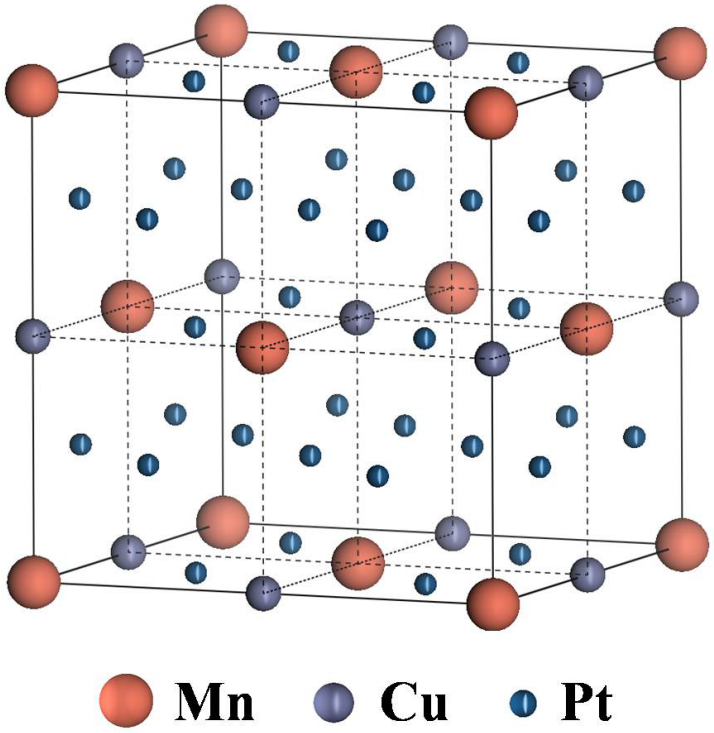

FIG. 1: Crystal structure of $CuMnPt_6$.

of two order parameters in the ABC_6 type structure utilizing the method of static concentration waves [10]. Magnetization measurements revealed that $CuMnPt_6$ exhibits a spin glass type magnetic behavior in its annealed state, and the corresponding temperature for freezing the magnetic moment is 40 K [11]. A high-temperature X-ray diffraction method was used to determine the thermal properties of $CuMnPt_6$, such as the Debye temperature, thermal expansion coefficients, and mean-square displacements of an atom [12]. The temperature dependence of the electrical resistivity of $CuMnPt_6$ were also studied, and it has a special low resistivity around 5.7×10^{-3} ohm m at room temperature [8].

In spite of these efforts, there are very limited experimental or theoretical data for the pressure derivative of the elastic and thermal properties of $CuMnPt_6$. Thus, it is highly desirable to perform such calculations. In this paper, the pressure effect on the structural, elastic, and thermal properties of $CuMnPt_6$ is studied by using *ab intio* density functional calculations. This research might contribute to some further understanding of the physical properties of the related platinum alloys in engineering.

II. DETAILS OF CALCULATION

Structural optimizations and properties calculations are performed using the Cambridge Serial Total Energy Package (CASTEP) [13] plane-wave basis set density functional theory (DFT) code. The effects of the exchange-correlation energy are treated within the generalized gradient approximation (GGA) [14] in the form of Predew-Burke-Ernzerhof (PBE) [15]. The cut off energy of the atomic wave functions is set to be 480 eV, and a 6×6×6 Monkhorst-Pack [16] grid of k-points is employed. Self-consistent field [17] calculations are implemented with a convergence criterion of 10^{-6} eV/atom on the total energy.

III. RESULTS AND DISCUSSION

III-1. Structural properties

The structural properties often hold the key to understanding the material properties from a microscopic point of view. In order to show how the structural parameters behave under pressure in $CuMnPt_6$, the equilibrium geometry of the unit cell is computed at fixed values of the applied hydrostatic pressure in the range of 0–60 GPa, where, at each pressure, a complete optimization for lattice constants is performed. The obtained lattice constant for $CuMnPt_6$ as a function of the applied pressure together with the experimental results [7] are plotted in Fig. 2. The inset shows the estimate of the temperature effect on the structural parameters. Notice that our calculated results are within 0.7% of experimental values, which indicate that the present calculations are reliable. Further, the calculated unit cell volumes at given pressure in the range of 0–60 GPa can be fitted well with a Vinet formulation [18]

$$P = 3K_0 x^{-2}(1-x)\exp\left[\frac{3}{2}(K_0'-1)(1-x)\right], \quad \text{with } x = (V/V_0)^{\frac{1}{3}}, \tag{1}$$

where K_0 and K_0' are the bulk modulus and its pressure derivatives, V_0 is the unit cell volume before deformation. The values of the fitted parameters for K_0 and K_0' are 241.3 GPa and 6.09, respectively.

III-2. Elastic properties

It is well known that the elastic constants determine the response of the crystal to external forces, which often provide valuable information about bonding characteristic, structural stability, brittleness or ductility, hardness, strength, etc. [19–21]. The calculated values of the three independent elastic constants (C_{11}, C_{12}, and C_{44}) for $CuMnPt_6$ at various pressures are plotted in Fig. 3. As can be seen, all the elastic constants increase with increasing pressure, but with quite different slopes and curvatures. The C_{11} shows nonlinear pressure dependencies, whereas C_{12} and C_{44} are almost linear with pressure. Unfortunately, there is little experimental or theoretical data for comparison with the present results. Future experimental measurements will test our calculated predictions. Notice that the requirement of mechanical stability under the isotropic pressure for cubic structure leads to

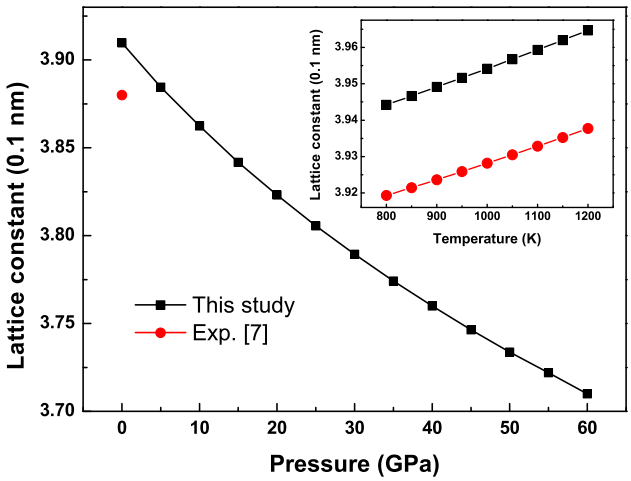

FIG. 2: The structural parameters of $CuMnPt_6$ varies with pressure and temperature.

the following conditions [22]: $(C_{11}+2C_{12}+P)/3 > 0$, $(C_{44}-P) > 0$, $(C_{11}-C_{12}-2P) > 0$. In our case, the elastic constants of $CuMnPt_6$ satisfy the above restriction equations, indicating that this compound is stable against elastic deformations.

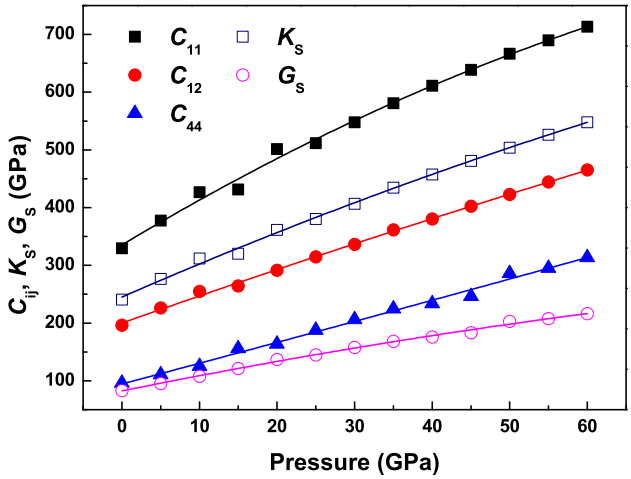

FIG. 3: Calculated pressure dependence of the elastic constants (C_{11}, C_{12}, and C_{44}), the bulk modulus (K_S), and the shear modulus (G_S) for $CuMnPt_6$.

It is usually assumed that the hardness of the materials is defined by the bulk modulus

and shear modulus: the former one represents the resistance to volume change by applied pressure, while the latter one represents the resistance to reversible deformations upon shear stress. Generally, the adiabatic bulk modulus K_S and shear modulus G_S of an isotropic polycrystalline can be obtained by means of the relations that $K_S = (C_{11} + 2C_{12})/3$ and $G_S = (G_V + G_R)/2$, where G_V and G_R are the Voigt averaged and Reuss averaged shear moduli, respectively [23–25]. The pressure dependencies of the aggregate elastic modulus (K_S, G_S) of $CuMnPt_6$ are presented in Fig. 3. It is found that the two parameters increase monotonically with the applied pressure, and the bulk modulus is sensitive to pressure as compared with the shear modulus. Moreover, the adiabatic bulk modulus K_S can be fitted well to a third-order finite strain equation of state [26]:

$$K_S = (1 + 2f)^{5/2} K_{0S}[1 + (3K'_{0S} - 5)f], \tag{2}$$

and the shear modulus G_S can be fitted well to a fourth-order finite strain equation of state:

$$G_S = G_{0S}(1+2f)^{5/2}\left\{1 + \left(3K_{0S}\frac{G'_{0S}}{G_{0S}} - 5\right)f + \frac{9}{2}\left[\left(\frac{K^2_{0S}}{G_{0S}}G''_{0S} + (K'_{0S} - 4)\frac{G'_{0S}}{K_{0S}}\right) + \frac{35}{9}\right]f^2\right\}, \tag{3}$$

where K_{0S}, K'_{0S}, G_{0S}, G'_{0S}, and G''_{0S} are the adiabatic bulk modulus, shear modulus, and their pressure derivatives (at zero pressure), f is the Eulerian strain, which is defined as $f = (x^2 - 1)/2$. The fitted values of the adiabatic bulk modulus K_{0S} and shear modulus G_{0S} at zero pressure are 240.8 GPa and 82.2 GPa, and their pressure derivatives K'_{0S}, G'_{0S} and G''_{0S} are 6.115, 2.857, and -0.012 GPa^{-1}, respectively. From Section III-1, we can see that the calculated values of the bulk modulus and its pressure derivatives from the elastic constants have nearly the same values as those obtained from the pressure-volume equation of states fitted by the Vinet formulation. This might be an estimate of the reliability and accuracy of our calculated elastic constants for $CuMnPt_6$.

The elastic anisotropy of a crystal is an important parameter, which is highly correlated with the possibility to induce microcracks in the materials [27]. To investigate the pressure effect on the elastic anisotropy of $CuMnPt_6$, the Zener ratio A_Z and the acoustic anisotropy factor A_a, which are defined as $A_Z = 2C_{44}/(C_{11} - C_{12})$ and $A_a = (2C_{44} + C_{12})/C_{11}$, are discussed in this study. The results are presented in Fig. 4. Generally, for an elastically isotropic material, both A_Z and A_a are equal to 1. As can be seen, the calculated value of A_Z at zero pressure is 1.44, and it increases almost linearly with pressure and finally reaches to 2.53 at 60 Gpa. While the calculated value of A_a increase from 1.18 at zero pressure to 1.53 at 60 GPa. The high-pressure behavior of A_Z is obviously caused by the smaller dependence on pressure of the tetragonal shear constant than that of the shear constant. One can show from the Cristoffel equation that for a cubic crystal, the acoustic velocity ratio $(v_{[111]}/v_{[100]})^2$ can be represented as $(1 + \beta A_a)$, where β is 2/3 for the P (longitudinal) wave and $-1/2$ or $-3/8$ for the two S (shear) waves [28, 29]. Then the results of A_a indicated that the difference between $v_{P[111]}$ and $v_{P[100]}$ ($v_{S[111]}$ and $v_{S[100]}$) is enhanced (declined) by pressurization. Both parameters exhibit that, in spite of

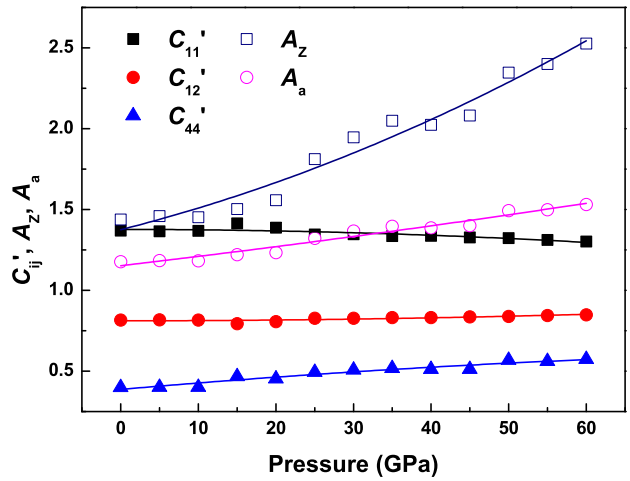

FIG. 4: Calculated pressure dependence of the normalized elastic constants (C'_{11}, C'_{12}, and C'_{44}), the Zener ratio (A_Z), and the acoustic anisotropy factor (A_a) for $CuMnPt_6$.

the cubic structure, $CuMnPt_6$ has a large elastic anisotropy even at zero pressure, and the elastic anisotropy increases with the applied pressure.

In order to investigate the elasticity of $CuMnPt_6$ in more detail, the normalized elastic constants C'_{ij}, which are defined by dividing a specific elastic constant with the bulk modulus [30], are studied and presented in Fig. 4. For an elastically ideal cubic crystal, namely the isotropic Cauchy solid, the values of C'_{11}, C'_{12}, and C'_{44} at zero pressure are 1.8, 0.6, and 0.6, respectively. Our results for the three parameters for $CuMnPt_6$ are 1.4, 0.8, and 0.4, respectively, which deviate from the ideal values. These deviations clearly connect with the elastic anisotropy. Further analysis shows that the C'_{ij} are almost independent of pressure or have only a small pressure dependence. The results are the same as that with the case of cubic system transition metals [31], but remarkably different from the case of alkaline earth oxides [29], which are also cubic crystal but strongly ionic compounds. This discussion may provide some more insight into the elasticity of intermetallic and ionic compounds; future work needs to be carried out more deeply.

III-3. Thermal properties

In order to compare our results with experiments, or predict what an experiment would yield for the thermal properties of $CuMnPt_6$, some representative parameters, such as the Debye temperature, Grüneisen constant, thermal expansion coefficient, and heat capacity, are calculated by using the quasi-harmonic Debye model [32, 33]. It is well known that the Debye temperature is a fundamental thermal parameter of a material, which is closely related to many physical properties, such as the specific heat, elastic constants, and melting point. The calculated pressure and temperature dependencies of the Debye

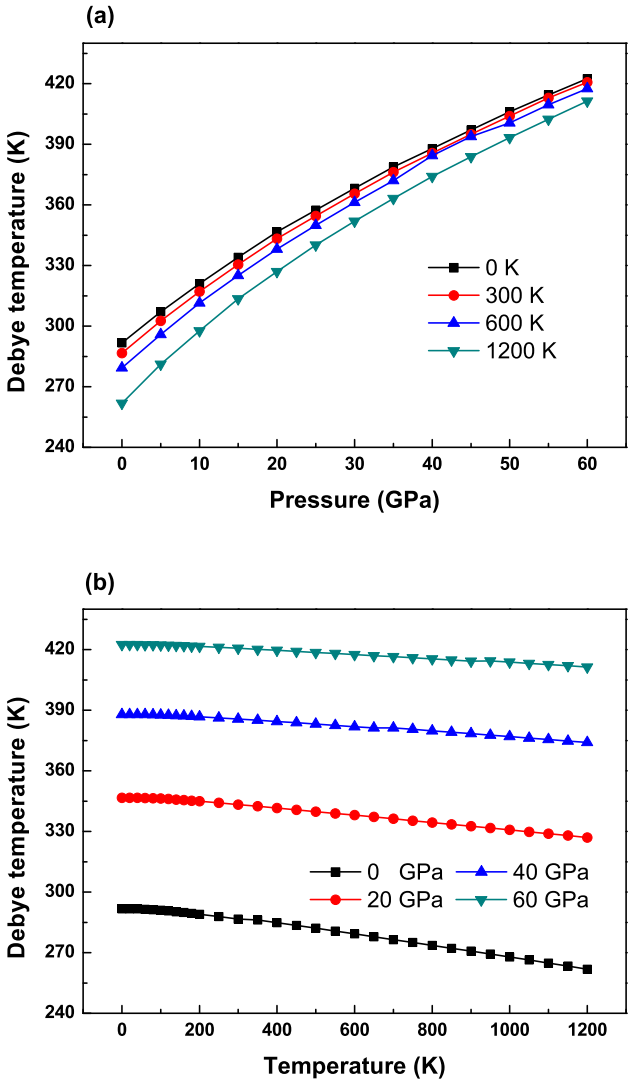

FIG. 5: The Debye temperature of $CuMnPt_6$ as a function of external conditions (T, P) under (a) different temperatures, and (b) different pressures.

temperature for $CuMnPt_6$ are presented in Fig. 5. Notice that our calculated Debye temperature for $CuMnPt_6$ at zero pressure and room temperature is 290 K, which is close to the corresponding experimental value 300 ± 9 K [18]. Further analysis shows that for a given temperature, the Debye temperature increases almost linearly with the applied pressure, and the dependence of the Debye temperature at different temperatures on pressure is roughly the same with only negligible discrepancies. While for a given pressure, the Debye temperature decreases almost linearly with increasing temperature, and the decreases are

10.2, 5.7, 3.6, and 2.6 % at the pressures of 0, 20, 40, and 60 GPa, respectively, when the temperature is from 0 to 1200 K. It is shown that its dependence on the temperature declined at higher pressure. The current investigations demonstrated that the Debye temperature exhibits strong pressure but weak temperature dependence.

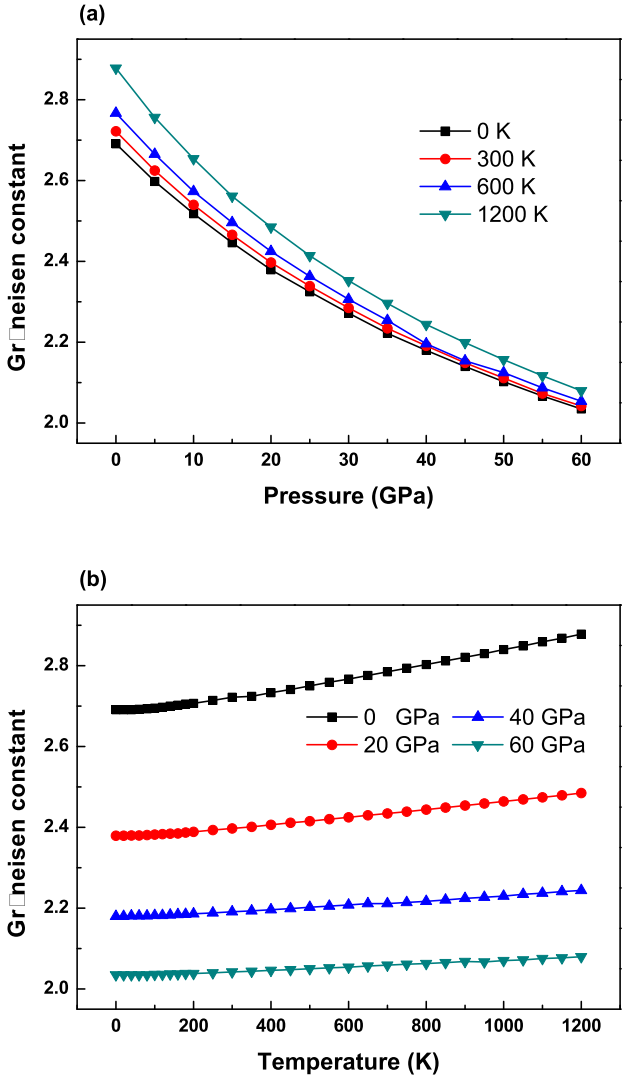

FIG. 6: The Grüneisen constant of $CuMnPt_6$ as a function of external conditions (T, P) under (a) different temperatures, and (b) different pressures.

It is usually assumed that the Grüneisen constant represents the degree of anharmonicity of the crystal lattice and relates to the thermal pressure. Our calculated results are shown in Fig. 6. It can be seen that at given temperature, the Grüneisen constant

decreases dramatically with pressure, and as the temperature goes higher, the Grüneisen constant decreases more rapidly with increasing pressure. While at fixed pressure, the Grüneisen constant increases monotonically with temperature, and the temperature dependence decreased at high pressure. The present results revealed that the anharmonicity decreases with pressure but increases with temperature.

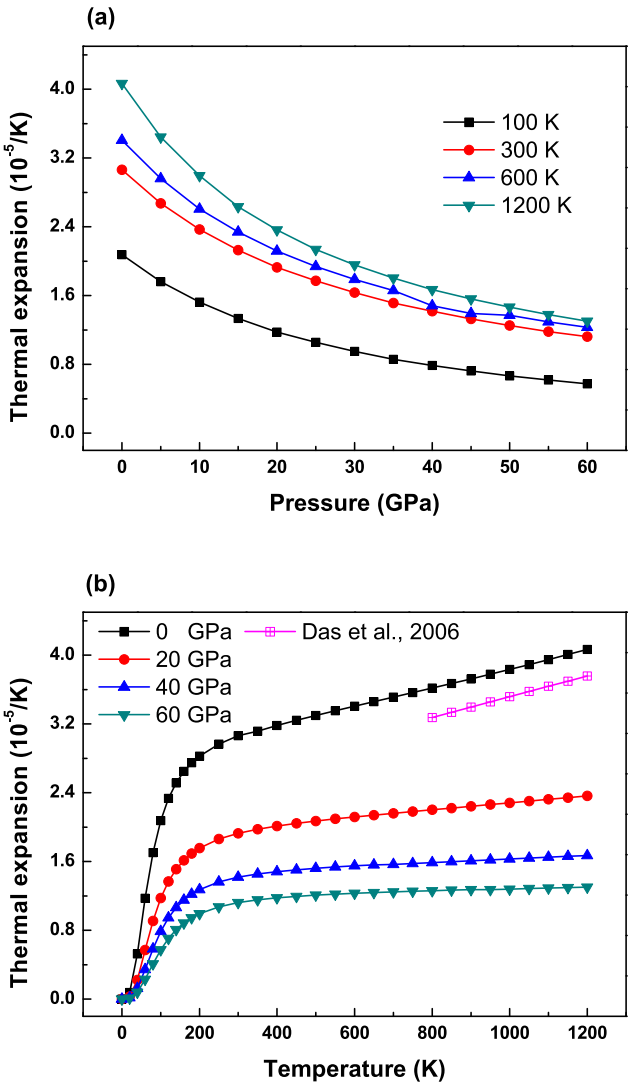

FIG. 7: The thermal expansion coefficient of $CuMnPt_6$ as a function of external conditions (T, P) under (a) different temperatures, and (b) different pressures.

The dependence of the thermal expansion with the pressure and temperature are presented in Fig. 7. Previous X-ray Debye-Scherrer measurements [7] of the thermal expansion

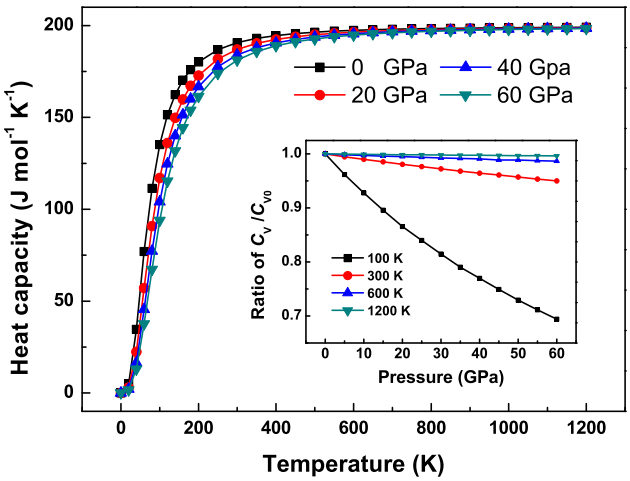

FIG. 8: The heat capacity of $CuMnPt_6$ varies with temperature under different pressures. The inset shows the ratio of C_V/C_{V0}, where C_V and C_{V0} are the heat capacity under any pressure P and zero pressure P_0 at the temperatures of 100, 300, 600, and 1200 K.

coefficient for $CuMnPt_6$ at zero pressure are also plotted for comparison. As can be seen, our results are slightly larger than the experimental values, but they have the same order of magnitude and a similar variation trend with an increase of temperature. Further analysis shows that the effects of pressure on the thermal expansion coefficient are very small at low temperature, whereas the effects quickly increase as the temperature increases. While for a given pressure, the thermal expansion coefficient increases rapidly at low temperatures and tends to be more gentle at higher temperature. It is known that the thermal expansion arises from anharmonic lattice dynamics and reflects the anharmonicity of the potential of crystal binding. Hence the nonlinearly changes of the thermal expansion coefficient with temperature have shown its anisotropic nature. Notice that both Figs. 6 and 7 have shown the same anharmonic inter-atomic potential of the crystal lattice.

Fig. 8 shows the relations of the heat capacity with temperature and pressure. It is immediately clear that when the pressure keeps constant, the values increase sharply with an increasing temperature at low temperature, at which it strictly follows the well-known T^3 law. And under high enough temperatures, the classical behavior of C_V-3R for mono-atomic solids is found, which obeys the Dulong-Petit limit rule. Further, the curves $C_V(T)$ decrease slightly with the applied pressure, and the pressure dependence remains very small at high temperature. In summary, the influences of temperature on the heat capacity are much more significant than pressure. However, due to the absence of corresponding experimental data for $CuMnPt_6$, the present results may be an attempt to predict the thermal properties, and a thorough understanding of its behavior is desirable.

IV. CONCLUSION

The application of first-principles calculations and the Debye model has permitted a detailed study of the structural, elastic, and thermal properties for the ABC_6-type $CuMnPt_6$ alloy. The calculated lattice parameter, Debye temperature, and thermal expansion coefficient are in good agreement with the corresponding experimental values. The C_{11}, C_{12}, and C_{44} obtained by using the static finite strain technique show a monotonic increase with pressure, while the normalized elastic constants are insensitive to pressure. Third- and fourth-order finite strain equations of state are applied to assess the bulk and shear modulus, respectively. The representative thermal parameters, including the Debye temperature, Grüneisen constant, thermal expansion coefficient, and heat capacity, as a function of temperature and pressure are calculated and discussed. The current investigations demonstrated that the anharmonicity decreases with pressure but increases with temperature. This study might contribute to the application of the related platinum alloy at high pressure and temperature.

Acknowledgements

This work is supported by the National Basic Research Program of China (Grant No. 2011CB606401).

References

[1] S. Imada *et al.*, Phys. Rev. B **59**, 8752 (1999).
[2] M. Carelse and C. I. Lang, Scripta Mater. **54**, 1311 (2006).
[3] P. M. Oppeneer *et al.*, Solid State Commun. **94**, 255 (1995).
[4] M. Takahashi, T. Sembiring, M. Yashima, T. Shishido, and K. Ohshima, J. Phys. Soc. Jpn. **71**, 681 (2002).
[5] T. Sembiring, M. Takahashi, K. Ota, T. Shishido, and K. Ohshima, J. Phys. Soc. Jpn. **71**, 2459 (2002).
[6] T. Káňa and M. Šob, Phys. Rev. B **85**, 214438 (2012).
[7] A. K. Das *et al.*, J. Phys. Soc. Jpn. **75**, 024604 (2006).
[8] M. Takahashi *et al.*, J. Alloy. Compd. **453**, 75 (2008).
[9] M. Takahashi *et al.*, J. Phys. Soc. Jpn. **75**, 013601 (2006).
[10] M. Takahashi, A. K. Das, T. Sembiring, H. Iwasaki, and K. Ohshima, Physica B **385–386**, 130 (2006).
[11] A. K. Das, A. Zakaria, and I. Kamal, J. Ban. Acad. Sci. **32**, 218 (2008).
[12] E. Ahmed, M. Takahashi, H. Iwasaki, and K. Ohshima, J. Alloy. Compd. **473**, 1 (2009).
[13] S. J. Clark *et al.*, Z. Kristallogr. **220**, 567 (2005).
[14] J. P. Perdew and Y. Wang, Phys. Rev. B **45**, 13244 (1992).
[15] J. P. Perdew, K. Burke, and M. Ernzerhof, Phys. Rev. Lett. **77**, 3865 (1996).
[16] H. J. Monkhorst and J. D. Pack, Phys. Rev. B **13**, 5188 (1976).
[17] P. Hohenberg and W. Kohn, Phys. Rev. **136**, B864 (1964).

[18] P. Vinet, J. Ferrante, J. H. Rose, and J. R. Smith, J. Geophys. Res. **92**, 9319 (1987).
[19] D. G. Clerc and H. M. Ledbetter, J. Phys. Chem. Solids **59**, 1071 (1998).
[20] S. Jhi, J. Ihm, S. G. Louie, and M. L. Cohen, Nature **399**, 132 (1999).
[21] P. Ravindran *et al.*, J. Appl. Phys. **84**, 4891 (1998).
[22] B. Holm, R. Ahuja, Y. Yourdshahyan, B. Johansson, and B. I. Lundqvist, Phys. Rev. B **59**, 12777 (1999).
[23] W. Voigt, Ann. Phys-Berlin **274**, 573 (1889).
[24] A. Reuss, Z. Angew. Math. Mech. **9**, 49 (1929).
[25] R. Hill, Proc. Phys. Soc. Sect. A **65**, 349 (1952).
[26] C. S. Zha, H. K. Mao, and R. J. Hemley, Proc. Natl. Acad. Sci. U.S.A. **97**, 13494 (2000).
[27] V. Tvergaard and J. W. Hutchinson, J. Am. Ceram. Soc. **71**, 157 (1988).
[28] B. B. Karki *et al.*, Am. Mineral. **82**, 51 (1997).
[29] T. Tsuchiya and K. Kawamura, J. Chem. Phys. **114**, 10086 (2001).
[30] L. Fast, J. M. Wills, B. Johansson, and O. Eriksson, Phys. Rev. B **51**, 17431 (1995).
[31] T. Tsuchiya and K. Kawamura, J. Chem. Phys. **116**, 2121 (2002).
[32] E. Francisco, J. M. Recio, M. A. Blanco, A. M. Pendás, and A. Costales, J. Phys. Chem. A **102**, 1595 (1998).
[33] M. A. Blanco, E. Francisco, and V. Luaña, Comput. Phys. Commun. **158**, 57 (2004).